

Controlling Large Electric Vehicle Charging Stations via User Behavior Modeling and Stochastic Programming

Alban Puech^{1,2,†}, Tristan Rigaut¹, William Templier¹, Maud Tournoud¹

¹ Schneider Digital — AI Hub, Schneider Electric, Grenoble, France

² École Polytechnique Fédérale de Lausanne (EPFL), Lausanne, Switzerland

alban.puech@epfl.ch

Abstract—This paper introduces an Electric Vehicle Charging Station (EVCS) model that incorporates real-world constraints, such as slot power limitations, contract threshold overruns penalties, or early disconnections of electric vehicles (EVs). We propose a formulation of the problem of EVCS control under uncertainty, and implement two Multi-Stage Stochastic Programming approaches that leverage user-provided information, namely, Model Predictive Control and Two-Stage Stochastic Programming. The model addresses uncertainties in charging session start and end times, as well as in energy demand. A user’s behavior model based on a sojourn-time-dependent stochastic process enhances cost reduction while maintaining customer satisfaction. The benefits of the two proposed methods are showcased against two baselines over a 22-day simulation using a real-world dataset. The two-stage approach demonstrates robustness against early disconnections by considering a wider range of uncertainty scenarios for optimization. The algorithm prioritizing user satisfaction over electricity cost achieves a 20% and 36% improvement in two user satisfaction metrics compared to an industry-standard baseline. Additionally, the algorithm striking the best balance between cost and user satisfaction exhibits a mere 3% relative cost increase compared to the theoretically optimal baseline — for which the nonanticipativity constraint is relaxed — while attaining 94% and 84% of the user satisfaction performance in the two used satisfaction metrics.

Index Terms—User Behavior Modeling, Stochastic Optimization, Electric Vehicles, Energy Efficiency

I. INTRODUCTION

The number of public electric vehicle (EV) charging stations (EVCS) has increased by 55% in 2022 [1], and this number is only expected to grow further as the EU and the US multiply incentives to support the development of publicly accessible fast-charging infrastructure [2], [3]. However, EV charging stations come with many challenges, both in their operation (e.g. load management, user access, payment, or compatibility) and in their integration into the existing electrical grids [4]. Additionally, EVCSs typically have to satisfy some power constraints, while satisfying the requests of their users and minimizing electricity costs. In this context, smart control

strategies are required and will play a key role in scaling the EVCS network.

The difficulty of EVCS control comes from the many uncertainties involved in their operation. While users can be asked to indicate their intended parking time, they often, in practice, disconnect their vehicles much before; creating a need for session-end forecasts. As EVCSs frequently run on contracts having penalties for consumption peaks, planning the charge requires modeling the arrival time, session duration, and energy requests of future sessions. This turns the problem of EVCS control into a stochastic optimization problem, which can be tackled using different Stochastic Optimization approaches.

In [5], Kai-Wen Cheng et al. propose an EV charging algorithm focused on minimizing carbon emissions while satisfying user requests. However, they do not address the issue of early disconnections and instead assume that the exact disconnection times are provided as input by users and are respected. This contrasts with our approach, which relies on predicting arrival and departure time scenarios, allowing us to satisfy user requests even in case of early disconnection, and to better model the future EVCS load. Additionally, their algorithm lacks constraints on maximum power delivery, which we account for to respect real-life operating conditions [6], [7]. In [8], Tucker et al. do model a transformer capacity constraint and forecast EV departures. However, departure scenarios are determined deterministically at the connection time of each EV. Similarly, future EV arrival times are obtained from a pre-computed daily model obtained by aggregating past charging session data, independently of past slot activity. On the contrary, our approach models connection and departure times as a function of sojourn times and includes additional features such as charging slot indices to capture slot-specific behaviors. Furthermore, while their heuristic enforces a certain charging rate for the first connection hour, our algorithm relies on customer satisfaction modeling embedded in the objective function to ensure satisfaction even in case of early disconnection. The need for charging session forecasting is discussed in [9], where the necessity arises from correcting user-declared information about expected disconnection times and modeling future station load. The use of machine learning algorithms for

[†] Work carried out while at Institut Polytechnique de Paris, Palaiseau, France

predicting EV charging behavior — including session duration, start, and end times — has also been explored in [10] and [11], that advocate for the incorporation of external data such as weather and traffic alongside historical charging data. In our approach, we build upon these insights to advance the modeling of charging behavior by generating connection and disconnection scenarios for stochastic optimization. However, we maintain a focus on utilizing locally available data, which aligns more closely with our implementation and deployment constraints, similar to the ones discussed in [12].

In this paper, we thus propose an approach that minimizes charging costs while preserving user satisfaction. The solution can easily be implemented on an industrial system and leverages the requests of the users while anticipating early disconnections. Our contributions are:

- An EVCS model that incorporates real-world constraints, such as slot power limitation, contract threshold overruns penalties, or early disconnection of EVs.
- A Two-Stage Stochastic Programming approach that utilizes charging session scenarios instead of a single forecast of future charging sessions.
- A modeling of the charging sessions’ end and start, formulated as a sojourn-dependent stochastic process, that improves the modeling approach presented in [12] and leverages user-provided information.
- A comparative analysis of our novel control method against two baselines in a simulation on a 22-day real-world dataset of an EVCS, comprising 32 slots.

In section II, we introduce the EVCS model with its dynamics and parameters. In section III, we state the EVCS control problem as a generic stochastic optimization problem. We describe the Multi-Stage-Stochastic Programming algorithms, along with our user behavior modeling, in IV. Finally, we present and discuss the numerical results obtained through simulations in section V.

II. EVCS MODEL

We model the EVCS as a discrete dynamical system. Control actions are taken at each time step t , of length Δt , from the sequence $\mathcal{T} = \{0, 1, \dots, T\}$. We denote by $n \in \mathbb{N}^*$ the number of slots. Slots are independent charging points that users connect their EVs to. The binary variable $o_t^i \in \{0, 1\}$ indicates whether the slot i , $i < n$ is in an “active” or “inactive” state at time $t \in \mathcal{T}$.

A. Charging session start

When a customer connects their EV to an “inactive” slot, they hand over a request to the slot controller, as per [13]. A request is a pair (k, δ) , where $k \in \mathbb{R}_{\geq 0}$ is the amount of electrical energy (kWh) to be provided to the EV — net of any transmission or charging loss — and $\delta \in \mathbb{N}^*$ is the announced parking time, expressed as a number of time steps. In practice, one can assume k to be directly given by the user, or obtained through an EV-companion app that either has access to the current state of charge of the EV or converts a mileage capacity request into an energy request. This connection starts a charging

session, and the associated slot state switches from “inactive” to “active”. The binary variable $a_t^i \in \{0, 1\}$ takes a positive value if slot i gets connected to an EV, receives a request, and thus switches from “inactive” to “active” state at time step t . This variable is activated only at connection time.

B. Charging session end

An “active” charging slot remains in its state until the charging session ends. A session end is triggered if the EV gets disconnected, **or if the announced parking time elapses**, even if the EV stays connected. Users may leave their EV connected to the slot longer than the announced end of parking time — resulting in idle time. The session end is thus designed in such a way that the controller cannot rely on this idle time to satisfy the user request, so as to discourage users from keeping their EV parked longer than initially indicated. We use the binary variable $q_t^i \in \{0, 1\}$ to indicate if a slot switches from an “active” to an “inactive” state at time t . At the controller level, there is no distinction between “inactive” slots that are still connected to an EV (e.g., after the announced parking time elapsed), and free slots.

C. Charging dynamics

At each time step $t \in \mathcal{T}$, an “active” slot i , $i < n$ can deliver an energy amount $e_t^i \leq \bar{e}$, $e_t^i \in \mathbb{R}_{\geq 0}$, where $\bar{e} \in \mathbb{R}_{>0}$ denotes the maximum energy amount that can be delivered by a slot in the span of a single time step. The remaining energy $r_t^i \in \mathbb{R}_{\geq 0}$ to provide the EV connected to the “active” slot i with, at time step t , is given by:

$$r_t^i = \begin{cases} k_t & \text{if } t = t_0 \\ r_{t-1}^i - \eta \cdot e_{t-1}^i & \text{if } t_0 < t \leq t_0 + \delta_{t_0}^i \end{cases} \quad (1)$$

where $\eta \in (0, 1]$ denotes the charge efficiency and $t_0 \in \mathcal{T}$ the time step during which the last request $(k_{t_0}^i, \delta_{t_0}^i)$ was made.

At each time step $t \in \mathcal{T}$, for each “active” slot i , considering a session with request $(k_{t_0}^i, \delta_{t_0}^i)$ starting at t_0 , we also introduce a variable z_t^i which stores the initial energy request of the session:

$$z_t^i = k_{t_0}^i \quad \forall t, t_0 \leq t \leq t_0 + \delta_{t_0}^i \quad (2)$$

This variable will prove useful later to measure the satisfaction of the users.

Finally, we store the remaining number of time steps from the current time step t before the announced end-of-parking time of slot i . We call this feature $m_t^i \in (\mathbb{N} \cup \{-\infty\})$. The variable takes value $-\infty$ for charging sessions that are predicted using our methodology described in section IV-C.

D. Costs and objectives

We control the EVCS in order to reach a trade-off between customer satisfaction and costs.

Customer satisfaction. We define the satisfaction score χ_t^i of an “active” slot i , $i < n$ using the ratio between the remaining energy r_t^i to provide to the EV, and the associated

initial energy requested $z_t^i = k_{t_0}^i$, where t_0 is the time step corresponding to the last connection:

$$\chi_t^i = 1 - \frac{r_t^i}{z_t^i} \quad (3)$$

Electricity costs. The EVCS consumption at time $t \in \mathcal{T}$ is denoted by $c_t \in \mathbb{R}_{\geq 0}$ and corresponds to the sum of the consumption of its slots. The electricity cost at time step t is denoted by $\zeta_t \in \mathbb{R}_{\geq 0}$ and is expressed as follows, with $p_t \in \mathbb{R}_{\geq 0}$ the electricity price at time t :

$$\zeta_t = p_t \times c_t \quad (4)$$

$$c_t = \sum_{i \in S} e_t^i \quad (5)$$

Grid import threshold overrun. At every time step $t \in \mathcal{T}$, a fixed penalty $\xi \in \mathbb{R}_{>0}$ is paid if the EVCS electricity consumption exceeds a threshold $\bar{c} \in \mathbb{R}_{>0}$, that is, if $c_t > \bar{c}$. At each time step t , the cost incurred by this threshold is then:

$$\mathbf{1}_{>\bar{c}}(c_t) \times \xi \quad (6)$$

where $\mathbf{1}_{>\bar{c}} : \mathbb{R} \rightarrow \{0, 1\}$ is the indicator function that takes the value 1 when its argument is above \bar{c} and 0 otherwise.

III. OPTIMAL CONTROL FORMULATION

We formulate hereunder the problem as a generic Stochastic Optimal Control problem using standard notations used in the Control literature [14].

A. State, exogenous uncertainty and control variables

The **state variable** at time $t \in \mathcal{T}$ is denoted by $x_t \in \mathbb{X} = (\{0, 1\} \times \mathbb{R}_{\geq 0} \times \mathbb{R}_{\geq 0} \times (\mathbb{N} \cup \{-\infty\}))^n$ and is expressed as:

$$x_t = (\underbrace{o_t^i}_{\substack{\text{state} \\ \in \\ \text{"active",} \\ \text{"inactive"}}, \underbrace{r_t^i}_{\substack{\text{remaining} \\ \text{energy} \\ \text{to provide}}}, \underbrace{z_t^i}_{\substack{\text{initial energy} \\ \text{request of} \\ \text{the session}}}, \underbrace{m_t^i}_{\substack{\text{remaining number} \\ \text{of steps before} \\ \text{announced end} \\ \text{of parking}}})_{i=0}^{n-1} \quad (7)$$

The **control (action)** at time $t \in \mathcal{T}$ is denoted by $u_t = (e_t^i)_{i=0}^{n-1}$ in the set $\mathbb{U} = (\mathbb{R}_{\geq 0})^n$ and gathers the power provided by each slot.

The **exogenous uncertainty variable** is denoted by $w_t \in \mathbb{W}$ where $\mathbb{W} = (\{0, 1\}^2 \times \mathbb{R}_{\geq 0} \times \mathbb{N}^*)^n$:

$$w_t = (\underbrace{a_t^i}_{\substack{\text{session} \\ \text{start} \\ \text{boolean}}}, \underbrace{q_t^i}_{\substack{\text{session} \\ \text{end} \\ \text{boolean}}}, \underbrace{k_t^i}_{\substack{\text{initial} \\ \text{kwh request}}}, \underbrace{\delta_t^i}_{\substack{\text{announced} \\ \text{parking} \\ \text{time}}})_{i=0}^{n-1} \quad (8)$$

The **constraints** and the **dynamics** are expressed as:

$$g_t(x_t, u_t, w_t) \leq 0 \quad (9)$$

$$x_{t+1} = f_t(x_t, u_t, w_t) \quad (10)$$

where $f_t : (\mathbb{X}, \mathbb{U}, \mathbb{W}) \rightarrow \mathbb{X}$ and $g_t : (\mathbb{X}, \mathbb{U}, \mathbb{W}) \rightarrow \mathbb{R}^{n_c}$ denote respectively the dynamics function and the constraints, and where n_c denotes the number of constraints.

We define the stage cost $L_t : (\mathbb{X}, \mathbb{U}) \rightarrow \mathbb{R}_{\geq 0}$ as a linear combination of the electricity cost (4), the grid threshold overrun penalty (6) and the satisfaction score (3), with weight

given to the satisfaction denoted $\alpha \in \mathbb{R}_{>0}$. This weight gives a monetary value to the satisfaction of the users.

$$L_t(x, u) = \underbrace{(\zeta_t + \mathbf{1}_{>\bar{c}}(c_t) \times \xi)}_{\text{electricity cost including penalties}} + \alpha \cdot \sum_{i < n} \underbrace{(1 - \chi_t^i)}_{\text{customer dissatisfaction}} \quad (11)$$

In general, this stage cost can depend on the exogenous uncertainties. We thus assume that L_t is a function mapping $(\mathbb{X}, \mathbb{U}, \mathbb{W})$ to $\mathbb{R}_{\geq 0}$.

B. Controller definition and Multi-Stage Stochastic Programming policies

Our goal is to define a control strategy or policy. A policy is a collection $\Phi = \{\phi_{t_0}\}_{t_0 \in \mathcal{T}}$ of mappings (one for each $t_0 \in \mathcal{T}$), that each takes a current state $x_{t_0} \in \mathbb{X}$, and an uncertainty history $h_{t_0} = \{w_t\}_{t \leq t_0}$, and that returns a control action $u_{t_0} \in \mathbb{U}$ satisfying the problem constraints:

$$\phi_{t_0} : (x_{t_0}, h_{t_0}) \mapsto u_{t_0} \in \{u \in \mathbb{U}, g_t(x_{t_0}, u_{t_0}, w_{t_0}) \leq 0\}$$

At time step t_0 , given a state x_{t_0} and a history h_{t_0} , a controller of policy Φ solves the following Multi-Stage Stochastic Programming problem and returns one of its solutions:

$$\arg \min_{u_{t_0} \in \mathbb{U}} \min_{(\mathbf{U}_{t_0+i})_{1 \leq i \leq R}} \mathbb{E} \sum_{t=t_0}^{t_0+R} L_t(\mathbf{X}_t, \mathbf{U}_t, \mathbf{W}_t) \quad (12a)$$

$$\text{s.t. } \mathbf{X}_{t+1} = f_t(\mathbf{X}_t, \mathbf{U}_t, \mathbf{W}_t) \quad (12b)$$

$$g_t(\mathbf{X}_t, \mathbf{U}_t, \mathbf{W}_t) \leq 0 \quad (12c)$$

$$\mathbf{X}_{t_0} = x_{t_0}, \mathbf{H}_{t_0} = h_{t_0} \quad (12d)$$

$$\sigma(\mathbf{U}_t) \subset \sigma(\mathbf{H}_{t_0}, \mathbf{W}_{t_0+1}, \dots, \mathbf{W}_t) \quad (12e)$$

where $R \in \mathbb{N}^*$ is a control horizon and where the expectation is computed over the conditional distribution of the uncertainties given the uncertainty history $\mathbb{P}(\mathbf{W}_{t_0}, \mathbf{W}_{t_0+1}, \dots, \mathbf{W}_{t_0+R} | \mathbf{H}_{t_0} = h_{t_0})$.

IV. METHODOLOGY

As the uncertainty distribution has infinite support, we solve the previously formulated problem on a limited number of uncertainty scenarios, obtained from a scenario tree. We thus have a tractable approximation of the expectation displayed in (12a). We here refer to [15] for further details about scenario trees, that conceptualize the strategy adopted here.

A. Multi-Stage Stochastic Programming algorithms

We use two Multi-Stage Stochastic Programming (MSSP) algorithms, namely, Two-Stage Stochastic Programming (2S) and Model Predictive Control (MPC).

1) *Two-stage Stochastic Programming (2S):* Two-stage Stochastic Programming uses a collection of $K \in \mathbb{N}^*$ samples indexed by $0 \leq k < K$ denoted $(w_{t_0}, \tilde{w}_{t_0+1}^k, \dots, \tilde{w}_{t_0+R}^k)_{k=0}^{K-1}$ drawn from the uncertainty distribution $\mathbb{P}(\mathbf{W}_{t_0}, \dots, \mathbf{W}_{t_0+R} | \mathbf{H}_{t_0} = h_{t_0})$, where the first variable of the sampled tuples, w_{t_0} , is observable and given by the history h_{t_0} and is thus fixed. These samples are then assigned to $K' \leq K$ clusters. The probability $\pi_k \in (0, 1]$ of a

cluster is then computed as the ratio between the number of samples associated with this cluster, and the total number of samples.

For each of the K' cluster centers, we find their closest sample, and we denote by $(w_{t_0}, \hat{w}_{t_0+1}^k, \dots, \hat{w}_{t_0+R}^k)_{k=0}^{K'-1}$ this new collection, that we then use to approximate the previously formulated problem by the following smaller and tractable optimization problem:

$$\arg \min_{u_{t_0} \in U} \min_{(u_t^k)_{t_0 < t \leq t_0+R} \atop k < K'} \sum_{t_0 \leq t \leq t_0+R} \pi_k \cdot L_t(x_t^k, u_t^k, \hat{w}_t^k) \quad (13a)$$

$$\text{s.t. } x_{t+1}^k = f_t(x_t^k, u_t^k, \hat{w}_t^k), \forall k < K', \forall t, t_0 \leq t < t_0 + R \quad (13b)$$

$$g_t(x_t^k, u_t^k, \hat{w}_t^k) \leq 0, \forall k < K', \forall t, t_0 \leq t \leq t_0 + R \quad (13c)$$

$$x_{t_0}^k = x_{t_0}, \forall k < K' \quad (13d)$$

2) *Model Predictive Control (MPC)*: Model Predictive Control uses a unique uncertainty forecast $(w_{t_0}, \hat{w}_{t_0+1}, \dots, \hat{w}_{t_0+R})$ of the future realizations of $(\mathbf{W}_{t_0}, \dots, \mathbf{W}_{t_0+R})$ conditioned by $\mathbf{H}_{t_0} = h_{t_0}$. In practice, the control action at time t_0 is thus obtained by solving the following optimization problem:

$$\arg \min_{u_{t_0} \in U} \min_{(u_t)_{t_0 < t \leq t_0+R}} \sum_{t_0 \leq t \leq t_0+R} L_t(x_t, u_t, \hat{w}_t) \quad (14a)$$

$$\text{s.t. } x_{t+1} = f_t(x_t, u_t, \hat{w}_t), \forall t, t_0 \leq t < t_0 + R \quad (14b)$$

$$g_t(x_t, u_t, \hat{w}_t) \leq 0, \forall t, t_0 \leq t \leq t_0 + R \quad (14c)$$

B. Uncertainty distribution modeling

In the following subsection, we explain how we model the uncertainty distribution, that we use to obtain the uncertainty samples used with 2S, and the uncertainty forecasts used with MPC.

1) *Session start and end*: We model the charging session state transition of each slot i , $i < n$ by a sojourn-dependent stochastic process \mathbf{O}^i with two possible states, $\mathbf{O}^i(t) = 0$ (inactive) or $\mathbf{O}^i(t) = 1$ (active). This formulation is inspired by the Sojourn-time-dependent semi-markov switching processes introduced in [16].

Sojourn-time-dependent semi-markov switching processes are semi-markov processes in which the switching (i.e. transition between two distinct states) probability depends on the sojourn time (i.e. the time elapsed since the last switch). In our approach, we additionally condition the switching probability on the following set of features, which we directly derive from the uncertainty history h_t :

- **Sojourn time (Number of time steps since the last state transition).** We keep track of the number of time steps since the last transition from “inactive” to “active” states, or from “inactive” to “active” states, in the variable $g_t^i \in \mathbb{N}$.
- **Time related-features.** An encoding of the current hour of the day, and the weekday, denoted by $l_t \in \mathbb{N}$.
- **Slot index.** Denoted \tilde{i} , $\tilde{i} < n$.

The transition probability $p_{y \rightarrow z}$ from state $y \in \{0, 1\}$ to state $z \in \{0, 1\}$ of slot i is thus defined as:

$$p_{y \rightarrow z}^i = \mathbb{P}\left(\mathbf{O}(t) = z \mid \mathbf{O}(t-1) = y, \underbrace{g = g_{t-1}^i}_{\text{sojourn time}}, l = l_{t-1}, \tilde{i} = i\right) \quad (15)$$

2) *kWh request*: We model the kWh request k_t^i as a deterministic function denoted \mathbf{k} of the sojourn time g , the time of the day l , and the slot index i : $\mathbf{k} : (\mathbb{N} \times \mathbb{N} \times \{0, 1, \dots, n-1\}) \rightarrow \mathbb{R}_{\geq 0}$.

C. Uncertainty distribution approximation

To approximate the uncertainty distribution and generate uncertainty samples $(w_{t_0}, \tilde{w}_{t_0+1}^k, \dots, \tilde{w}_{t_0+R}^k)_{k=0}^{K-1}$, we use a training dataset containing past charging sessions to fit two gradient-boosting classifiers and a regressor. These are then used to obtain each of the uncertainty components:

- **Session starts.** The first classifier c_1 is used to obtain the transition probabilities from “inactive” to “active” state, so as to obtain the session start uncertainty samples denoted $(a_{t_0}, \tilde{a}_{t_0+1}, \dots, \tilde{a}_{t_0+R})$. It approximates the distribution $p_{0 \rightarrow 1}^i = \mathbb{P}(\mathbf{O}(t) = 1 \mid \mathbf{O}(t-1) = 0, g = g_{t-1}^i, l = l_{t-1}, \tilde{i} = i)$ conditioned by the previous slot activation state, the sojourn time, the time and date, and the slot index.
- **Kwh requests.** The regressor r_1 is used to obtain the kWh request associated with a session start (transition from “inactive” to “active” state). It approximates \mathbf{k} , the function that returns the kWh requests given (g, l, \tilde{i}) , as defined in IV-B2. Note that δ_t^i , the announced parking time associated with a session start on slot i at time t is not predicted. This approach yielded better results than the one based on session end prediction. Consequently, the remaining number of time steps before the announced disconnection of EV connected to slot i , m_t^i is set to $-\infty$ as a flag.
- **Session ends.** The second classifier is used to obtain the transition probabilities from the “active” to “inactive” state, and thus, the session end uncertainty samples $(q_{t_0}, \tilde{q}_{t_0+1}, \dots, \tilde{q}_{t_0+R})$. It approximates: $p_{1 \rightarrow 0}^i = \mathbb{P}(\mathbf{O}(t) = 0 \mid \mathbf{O}(t-1) = 1, g = g_{t-1}^i, l = l_{t-1}, \tilde{i} = i)$

Algorithm 1 is used to generate the uncertainty samples using c_1, c_2 and r_1 ; its working principle is illustrated in Fig. 1.

This modeling shows numerous improvements over the one introduced in [12]. Regarding the end-of-session times, our novel model allows for correcting the tendency of users to disconnect their vehicles before the announced end of parking time, while [12] was assuming this announced time to be the effective end-of-session time. In [12], the controller could plan on charging the EVs on the very last time steps of the announced parking period, which would lead to customer dissatisfaction if the users disconnected their EVs earlier. By allowing our model to predict session ends to happen before the expected time, this risk is reduced.

Moreover, as opposed to the heuristic proposed in [12] consisting in setting the load of free slots to constant values to simulate future charging sessions; planning the sessions start, sessions end, and kWh request allows for more accurate modeling of the future EVCS load.

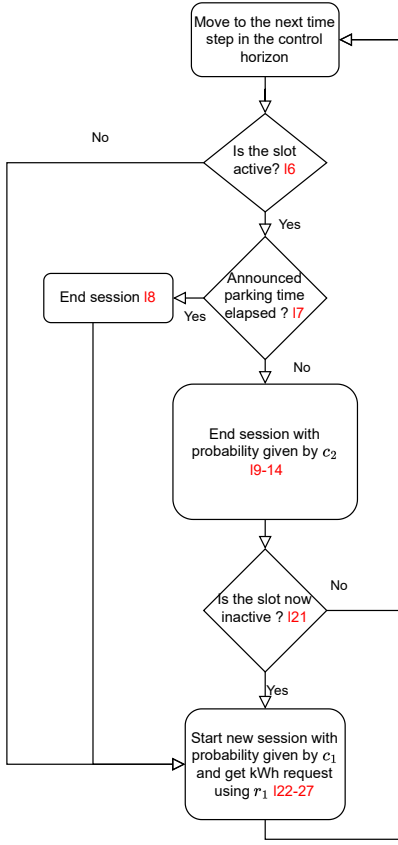


Fig. 1. Working principle of a single iteration of the scenario generation algorithm on a single charging slot. The text in red indicates the corresponding lines in the code of Algorithm 1

D. Uncertainty forecasts for MPC

To obtain different uncertainty samples (used with 2S), the switches between states are done with probability obtained using c_1 and c_2 , allowing different scenarios to be obtained for the same state conditions. As introduced in IV-A2, our MPC algorithm uses an uncertainty forecast instead of relying on a collection of uncertainty samples. In this context, the switch between states is done in a deterministic way, i.e. only if the probability of state switch (obtained using c_1 and c_2) is greater than the probability of staying in the same state. In practice, this means that lines 13, and 25 are modified to compare p with 0.5 instead of a random value.

E. Baseline algorithms

We compare our two MSSP algorithms (MPC and 2S) against two baselines.

Algorithm 1 Uncertainty sample drawing: Draw a sample of the future uncertainties $(w_{t_0}, \tilde{w}_{t_0+1}, \dots, \tilde{w}_{t_0+R})$ from $\mathbb{P}(\mathbf{W}_{t_0}, \mathbf{W}_{t_0+1}, \dots, \mathbf{W}_{t_0+R} | \mathbf{H}_{t_0} = h_{t_0})$

```

1: function GET_SAMPLE( $x_{t_0}, h_{t_0}$ )
2:   for  $t \in [t_0 + 1 \dots t_0 + R]$  do
3:      $g_{t-1}, m_{t-1}, l_{t-1}, a_{t-1}, \delta_{t-1} \leftarrow \text{GET\_FEATURES}(h_{t-1})$  ▷ Compute features from uncertainty history
4:     for  $i, i < n$  do
5:        $o_t^i \leftarrow o_{t-1}^i$  ▷ set current state to be the previous one by default
6:       if  $o_t^i = 1$  then ▷ if slot  $i$  was in active state...
7:         if  $m_{t-1}^i = 0$  then
8:            $o_t^i \leftarrow 0$  ▷ end session if announced parking time elapsed
9:         else ▷ if announced parking time has not elapsed...
10:           $p \leftarrow c_2(g_{t-1}, l_{t-1}, i)$ 
11:          if  $\text{RANDOM.RAND}() < p$  then ▷ end session with probability  $p$ 
12:             $o_t^i \leftarrow 0$ 
13:          end if
14:        end if
15:         $h_t \leftarrow \text{UPDATE\_HISTORY}(g_{t-1}, m_{t-1}, l_{t-1}, a_{t-1}, \delta_{t-1}, o_t)$  ▷ update history
16:      end if
17:    end for
18:
19:     $g_t, m_t, l_t, a_t, \delta_t \leftarrow \text{GET\_FEATURES}(h_t)$  ▷ Update features from uncertainty history
20:    for  $i, i < n$  do
21:      if  $o_t^i = 0$  then ▷ if slot was in inactive state (or has just transitioned to inactive state)...
22:         $p \leftarrow c_1(g_t, l_t, i)$ 
23:        if  $\text{RANDOM.RAND}() < p$  then ▷ start session with probability  $p$ 
24:           $o_t^i \leftarrow 1$ 
25:           $k_t^i \leftarrow r_1(g_t, l_t, i)$  ▷ get kWh request
26:           $m_t^i \leftarrow -\infty$  ▷ set announced parking time duration to  $-\infty$  (as a flag)
27:        end if
28:      end if
29:    end for
30:
31:     $h_t \leftarrow \text{UPDATE\_HISTORY}(g_t, m_t, l_t, a_t, \delta_t, o_t)$ 
32:  end for
33:   $(w_{t_0}, \tilde{w}_{t_0+1}, \dots, \tilde{w}_{t_0+R}) \leftarrow h_{t_0:t_0+R}$ 
34:  return  $(w_{t_0}, \tilde{w}_{t_0+1}, \dots, \tilde{w}_{t_0+R})$ 
35: end function
  
```

1) *User request-based MPC (R-MPC)*: The first one, which we call R-MPC is a Model Predictive Control approach that solely relies on the user requests to build the uncertainty forecast. It is the algorithm introduced in [12]. The user-announced end-of-parking time is **assumed to be true** and **no modeling of the future charging session start and end is done**. Instead, the load on empty slots is replaced by an uncontrollable average energy consumption given the time of the day and the slot identifier. These average energy consumption values are obtained by running P-MPC (as defined in the next section) on a training set. We recall the expression of the exogenous uncertainties:

$$w_t = (\underbrace{a_t^i}_{\text{session start}}, \underbrace{q_t^i}_{\text{session end}}, \underbrace{k_t^i}_{\text{initial kWh request}}, \underbrace{\delta_t^i}_{\text{announced parking time}})_{i=0}^{n-1}, \quad (16)$$

The session ends of currently “active” slots are computed using the announced parking times. Moreover, no future session is predicted, so that $a_t^i = k_t^i = \delta_t^i = 0 \forall t, t_0 + 1 \leq t \leq t_0 + R$.

Assuming that slot i is “active” and that the last request

$r_{t_0}^i = (k_{t_0}^i, \delta_{t_0}^i)$, we get:

$$q_t^i = \begin{cases} 1 & \text{if } t = t_0 + \delta_{t_0}^i, \\ 0 & \text{if } t \neq t_0 + \delta_{t_0}^i \end{cases} \quad (17)$$

This baseline is the most straightforward MPC approach that can be deployed using the available user data. However, it does not anticipate the end of charging sessions by disconnections happening before the announced parking time elapses and does not account for potential future charging sessions that could increase the load in future time steps, as it only uses an average load. This becomes problematic if the EVCS delays the charge of the current EVs on those time steps — e.g., because of off-peak prices, for example — as it results in unsatisfied charging requests.

2) **P-MPC: Perfect MPC**: The second baseline, called P-MPC, is an MPC algorithm for which the nonanticipativity constraint is relaxed. In practice, this means that it is given the true realizations of the random variables as forecast.

V. RESULTS

We present numerical results obtained by implementing the previously presented algorithms and running them on a smart charging simulator based on real EV charging data.

A. Experiment setup

1) **Datasets**: We use the Caltech Adaptive charging network dataset [17]. This dataset contains charging session logs with duration, connection and disconnection time, kWh request, announced parking duration, and slot identifiers.

The portion used for training covers 83 days and contains 1123 sessions across $n = 32$ slots. Each slot has at least 20 training sessions. The one used for testing covers 22 days, and contains 352 sessions over the same number of slots.

The dataset is pre-processed to obtain fixed interval data points of $\Delta t = 15$ min. Connection and disconnection times are rounded to the nearest quarter-hour, and the charging session information is encoded using the uncertainty variables introduced in section II.

Unsatisfiable user requests are rounded down to the largest amount of energy that can be provided in the span of the announced parking time. This means that all requests can be satisfied if the users let their EV connected to the slot for the parking duration that they anticipated. However, this does not always happen in practice. **These early disconnections are responsible for P-MPC not being able to reach 100% satisfaction.**

2) **EVCS settings**: The EVCS parameters are of an existing EVCS station. We set the maximum slot power to 12kW. Each slot can thus deliver an energy amount equal to $\bar{e} = 3$ kWh in the span of one time step (15 minutes). We further set the subscribed power limit to 8% of the total nominal capacity of the EVCS, i.e. $\bar{c} = 0.08 \cdot n \cdot \bar{e} = 7.68$ kWh per time step. This corresponds to two times the average EVCS load. The electricity prices are set to 0.102€ during off-peak hours (i.e. from 00:00 to 06:00, 09:00 to 11:00, 13:00 to 17:00, and 21:00 to 00:00) and to 0.153€ during peak hours. Similarly, the

threshold overrun penalty is set to $\xi = 14.31$ € for every time step spent above the threshold, as per the “Tarif Jaune” rate from France’s main electric utility company EDF [18]. Finally, the battery charge efficiency of the connected EVs is set to $\eta = 0.91$

B. Implementation specifics

We run all algorithms on the test dataset with a control horizon $R = 40$. 2S uses $K' = 2$ uncertainty scenarios obtained from a total of $K = 20$ samples. We model the optimization problems with Pyomo [19] and solve them using HiGHS [20]. The classification and regression models described in IV-C are implemented using CatBoost [21].

C. Evaluation metrics

The algorithms are compared based on the following criteria:

- **Electricity costs**: Total cost of electricity, including the contract threshold overrun penalties.
- **Satisfaction metrics**:
 - **Filling rate**: What percentage of the user request is provided on average by the end of the session.
 - **Full satisfaction rate**: Percentage of requests that are fully satisfied (an energy amount corresponding to the initial request has been provided) at the end of session time.

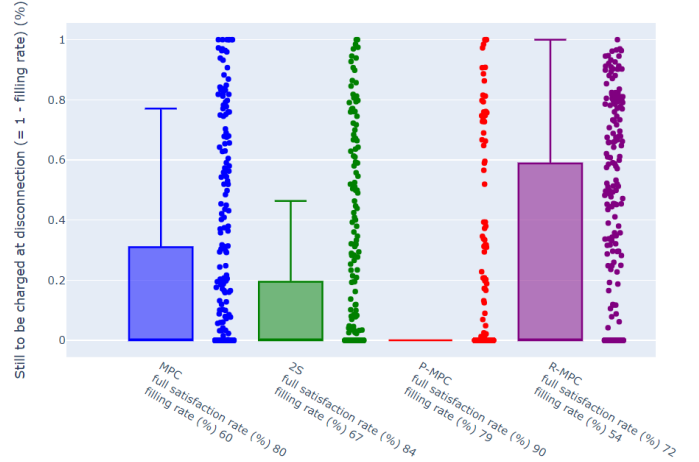


Fig. 2. Distribution of the share of the initial energy request that could not be provided by the end of the charging sessions. $\alpha = 5000$

D. Results

We report in Table I the results obtained for different α , the weight given to the satisfaction component of the objective function:

For small α (low penalization of unsatisfied requests), the filling and full-satisfaction rates are low but identical across all algorithms except R-MPC, which shows lower values. The electricity cost with MPC and 2S are larger than those obtained with P-MPC, which could be explained by the fact that these algorithms can not plan the charging sessions as well as P-MPC, and hence can not benefit from the off-peak hours as much.

TABLE I

SIMULATION RESULTS. THE RESULTS IN BOLD CORRESPOND TO THE VERSION OF 2S THAT OFFERS THE CLOSEST RESULTS TO P-MPC, WHILE ACHIEVING HIGH SATISFACTION RATES

α	Alg.	Objective	Electricity cost (EUR)	Filling rate (%)	Full satisfaction rate (%)	Electricity cost relative difference w.r.t P-MPC (%)	Filling rate relative difference w.r.t P-MPC (%)	Full satisfaction relative difference w.r.t P-MPC (%)
500	2S	99056	12991	69%	60%	16%	3%	-1%
500	MPC	98600	12392	68%	59%	10%	1%	-2%
500	R-MPC	177245	32942	70%	52%	194%	4%	-14%
1000	2S	139141	17286	77%	66%	3%	-4%	-9%
1000	MPC	139401	17156	77%	65%	-4%	-5%	-10%
1000	R-MPC	222683	34519	72%	53%	93%	-10%	-26%
5000	2S	404811	43094	85%	67%	3%	-6%	-16%
5000	MPC	445859	38484	81%	61%	-8%	-10%	-23%
5000	R-MPC	564019	37859	73%	55%	-9%	-19%	-31%
50000	2S	1744329	138893	92%	83%	122%	-1%	-2%
50000	MPC	2097777	117179	89%	78%	87%	-4%	-7%
50000	R-MPC	4214607	45470	74%	54%	-27%	-21%	-36%

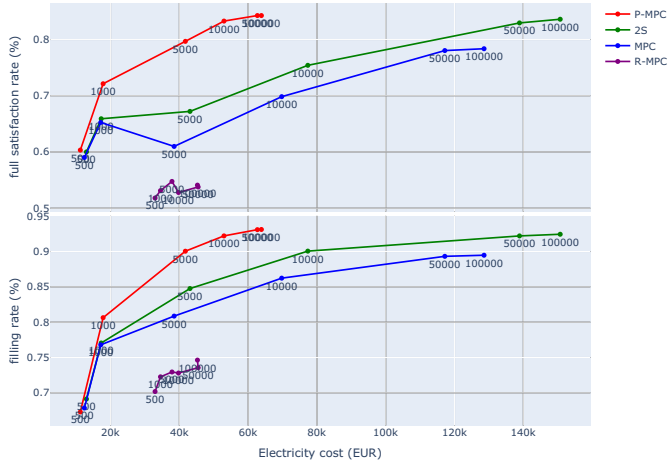


Fig. 3. Full satisfaction and filling rates as a function of the electricity costs. text annotations correspond to the values of α

As the value of α increases ■, the two satisfaction metrics both increase for all algorithms, and our 2S and MPC algorithms show very similar results to P-MPC. For $\alpha = 5000$, 2S is only 3% more costly but achieves 94% of the performance of P-MPC in terms of filling rate, and 84% in terms of full satisfaction rate. These values are respectively 16% and 23% higher than the ones obtained with our industry-grade baseline R-MPC.

As the value of α gets very large ■, the results obtained by 2S are close to the ones obtained with P-MPC in terms of satisfaction, while those obtained with MPC are slightly lower. With $\alpha = 10^5$, The filling rates of 2S and P-MPC are almost identical (92% for 2S against 93% for P-MPC), and the full satisfaction rates are equal (84% for both algorithms). 2S improves the filling rate obtained using R-MPC, our industry-grade baseline by 24%, and the full satisfaction rate by 55%. The electricity costs are significantly higher for both MPC and 2S (respectively 101% and 136% higher than with P-MPC), as customer unsatisfaction is much more penalized than electricity costs. Note that the fact that P-MPC does not reach 100% of satisfaction rate is because of early disconnections of sessions that could could otherwise been satisfied.

Fig. 3 demonstrates that 2S is more robust than MPC in terms

of customer satisfaction, as it achieves higher values for both satisfaction metrics. This can be attributed to the fact that the control action is derived from a greater number of uncertainty scenarios, increasing the likelihood of anticipating early session ends caused by early disconnections. Consequently, the controller is incentivized to initiate charging earlier and at a higher charging rate in these situations. Additionally, 2S achieves higher satisfaction scores than MPC for the same electricity costs, positioning itself as the best-performing algorithm that can be realistically implemented. Moreover, 2S significantly improves the results obtained by MPC for every value of α . The improvements of 2S over R-MPC are particularly significant for large values of α , for which the full satisfaction rate of 2S is 55% higher than the one obtained with R-MPC.

Finally, we show in Fig. 2 the distribution of the percentage of the initial request that was left to be provided at disconnection time, for the different algorithms with $\alpha = 5000$. R-MPC shows the largest values, as it uses the announced end of session time without correcting the user bias, so that many EVs get disconnected before they receive the requested energy amount. In average for $\alpha = 5000$, P-MPC, 2S, MPC and R-MPC respectively took 164ms, 1563ms, 556ms, and 193ms per time step on a modern laptop with an Intel i7 1185G7.

VI. CONCLUSION

In this paper, we presented an Electric Vehicle Charging Station (EVCS) model that considers numerous real-world constraints, including slot power limitations, penalties for contract threshold overruns, and early disconnections of EVs. We proposed a mathematical formulation for the optimal control problem under uncertainty and implement two Multi-Stage Stochastic Programming approaches: Model Predictive Control and Two-Stage Stochastic Programming. These approaches leverage the information provided by EV users. The problem complexity arises from uncertainties in charging session start and end times, as well as the energy requested by users. This necessitates predicting future charging session times and their energy demand. Early disconnections pose an additional challenge, as customers may disconnect their EVs before the initially announced time, further complicating charge planning. To address this, we introduced a user behavior model based on

a sojourn time-dependent stochastic process that considers the duration of the charging session, allowing for cost reduction while maintaining customer satisfaction.

Our algorithms were compared to two baselines: a Model Predictive Control algorithm with a perfect forecast of the future uncertainties (P-MPC), representing a theoretical optimal controller, and an industry-grade Model Predictive Control algorithm mentioned in [12]. Simulations were conducted using a real-world dataset spanning 22 days. The results demonstrated the advantages of our methods, which incorporate user behavior modeling and leverage user-provided information. Particularly, the Two-Stage Stochastic Programming method proves robust against early disconnections by considering a greater number of uncertainty scenarios for optimization. Our Two-Stage algorithm, prioritizing user satisfaction over electricity cost, performs comparably to the optimal baseline, outperforming our previous algorithm from [12] by 24% and 55% in the two user satisfaction metrics, respectively. The algorithm that strikes the best balance between cost and user satisfaction shows a 3% relative cost difference (slightly higher) compared to the optimal baseline, while achieving 94% and 84% of the user satisfaction performance of the optimal baseline in the two metrics used.

In the near future, we plan on studying the performance of our algorithm on charging sessions for which no end-of-parking time was specified by the user. Another major addition to this work would be to add a second optimization layer that would take advantage of the idle time (the period when an EV is still connected, although the announced end of parking time has elapsed) to complete the charge of the EVs that could not be charged on time. Finally, future work will also consist in incorporating EVCS control into the control of a larger microgrid that additionally features battery storage systems and PV production. This transition aims to move beyond solving local optimization problems towards establishing broader control systems and will require combining EV behavior modeling, battery charge scheduling [22], and netload modeling [15].

ACKNOWLEDGMENTS

The authors sincerely thank Claude Lepape, Jean-Christophe Alais, and Alejandro Yousef Da Silva for their valuable input and support.

REFERENCES

- [1] IEA, “Trends in charging infrastructure – global ev outlook 2023 – analysis,” 2023. [Online]. Available: <https://www.iea.org/reports/global-e-v-outlook-2023/trends-in-charging-infrastructure>
- [2] J. O. of Energy and Transportation, “State plans for electric vehicle charging,” 2022. [Online]. Available: <https://driveelectric.gov/state-plans/>
- [3] EIB, “Europe’s alternative fuels infrastructure getting a boost from new eib and european commission support,” 2021. [Online]. Available: <https://www.eib.org/en/press/all/2021-339-europe-s-alternative-fuels-i-infrastructure-getting-a-boost-from-new-eib-and-european-commission-n-support>
- [4] M. Mastoi, S. Zhuang, H. Munir, M. Haris, M. Hassan, M. Usman, S. Bukhari, and J. Ro, “An in-depth analysis of electric vehicle charging station infrastructure, policy implications, and future trends,” *Energy Reports*, vol. 8, pp. 11 504–11 529, 2022. [Online]. Available: <https://www.sciencedirect.com/science/article/pii/S2352484722017346>
- [5] K.-W. Cheng, Y. Bian, Y. Shi, and Y. Chen, “Carbon-aware ev charging,” in *2022 IEEE International Conference on Communications, Control, and Computing Technologies for Smart Grids (SmartGridComm)*, 2022, pp. 186–192.
- [6] S. Powell, E. C. Kara, R. Sevlian, G. V. Cezar, S. Kilicotte, and R. Rajagopal, “Controlled workplace charging of electric vehicles: The impact of rate schedules on transformer aging,” *Applied Energy*, vol. 276, p. 115352, 2020. [Online]. Available: <https://www.sciencedirect.com/science/article/pii/S0306261920308643>
- [7] M. Muratori, “Impact of uncoordinated plug-in electric vehicle charging on residential power demand,” *Nature Energy*, vol. 3, no. 3, pp. 193–201, 2018.
- [8] N. Tucker, G. Cezar, and M. Alizadeh, “Real-time electric vehicle smart charging at workplaces: A real-world case study,” in *2022 IEEE Power & Energy Society General Meeting (PESGM)*, 2022, pp. 1–5.
- [9] E. Genov, C. D. Cauwer, G. V. Kriekinge, T. Coosemans, and M. Messagie, “Forecasting flexibility of charging of electric vehicles: Tree and cluster-based methods,” *Applied Energy*, vol. 353, p. 121969, 2024. [Online]. Available: <https://www.sciencedirect.com/science/article/pii/S0306261923013338>
- [10] S. Shahriar, A. R. Al-Ali, A. H. Osman, S. Dhou, and M. Nijim, “Machine learning approaches for ev charging behavior: A review,” *IEEE Access*, vol. 8, pp. 168 980–168 993, 2020.
- [11] ———, “Prediction of ev charging behavior using machine learning,” *IEEE Access*, vol. 9, pp. 111 576–111 586, 2021.
- [12] T. Rigaut, A. Yousef, M. Andreeva, and V. Ignatova, “Scalable forecasting and model predictive control for electric vehicles smart charging,” in *CIRED Porto Workshop 2022: E-mobility and power distribution systems*, vol. 2022, Porto, Portugal, 2022, pp. 893–897.
- [13] ISO, “Iso 15118-1:2019 road vehicles — vehicle to grid communication interface — part 1: General information and use-case definition,” 2019. [Online]. Available: <https://www.iso.org/standard/69113.html>
- [14] D. Bertsekas, *Dynamic programming and optimal control: Volume 1*. Athena scientific, 2012, vol. 1.
- [15] A. Puech, T. Rigaut, A. L. Franc, W. Templier, J.-C. Alais, M. Tournoud, V. Bossard, A. Yousef, and E. Stolyarova, “Controlling microgrids without external data: A benchmark of stochastic programming methods,” in *2023 IEEE PES Innovative Smart Grid Technologies Europe (ISGT EUROPE)*, 2023, pp. 1–5.
- [16] L. Campo, P. Mookerjee, and Y. Bar-Shalom, “State estimation for systems with sojourn-time-dependent markov model switching,” *IEEE Transactions on Automatic Control*, vol. 36, no. 2, pp. 238–243, 1991.
- [17] Z. Lee, T. Li, and S. Low, “ACN-Data: Analysis and Applications of an Open EV Charging Dataset,” in *Proceedings of the Tenth International Conference on Future Energy Systems*, ser. e-Energy ’19, Jun. 2019.
- [18] J. officiel de la république Française, “Arrêté du 30 juillet 2015 relatif aux tarifs réglementés de vente de l’électricité,” Jul 2015. [Online]. Available: http://www.energies-services.org/upload/ccc29_arrete2015.pdf
- [19] M. Bynum, G. Hackebeil, W. Hart, C. Laird, B. Nicholson, J. Siiriola, J. Watson, and D. Woodruff, *Pyomo—optimization modeling in python*, 3rd ed. Springer Science & Business Media, 2021, vol. 67.
- [20] Q. Huangfu and J. J. Hall, “Parallelizing the dual revised simplex method,” *Mathematical Programming Computation*, vol. 10, no. 1, pp. 119–142, 2018.
- [21] L. Prokhorenkova, G. Gusev, A. Vorobev, A. Dorogush, and A. Gulin, “Catboost: unbiased boosting with categorical features,” 2019.
- [22] A. Puech, G. Dimitrov, and C. D’Ambrosio, “Optimal battery charge scheduling for revenue stacking under operational constraints via energy arbitrage,” in *2023 IEEE PES Innovative Smart Grid Technologies Europe (ISGT EUROPE)*, 2023, pp. 1–5.